

Supplementary Material

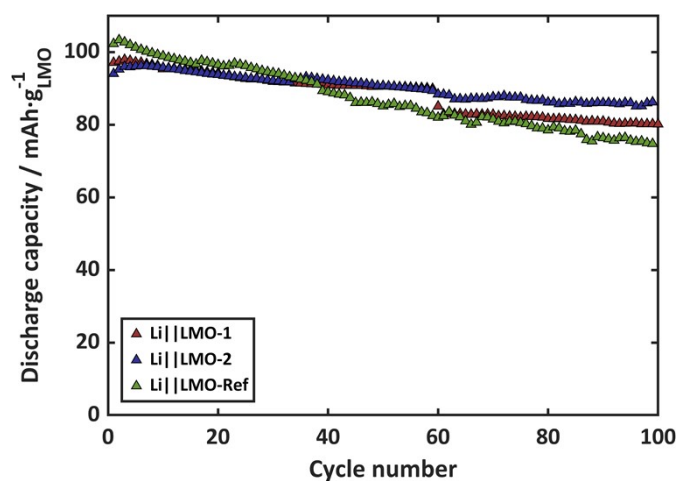


Figure S1: Graphs for the comparison between the commercial PVDF-based LMO-cathode (LMO-Ref) and the F-free PIB-based LMO cathodes (LMO-1 and LMO-2) cycled in a half-cell configuration. Cycling data is presented as the mean value of two representative cells for each configuration.

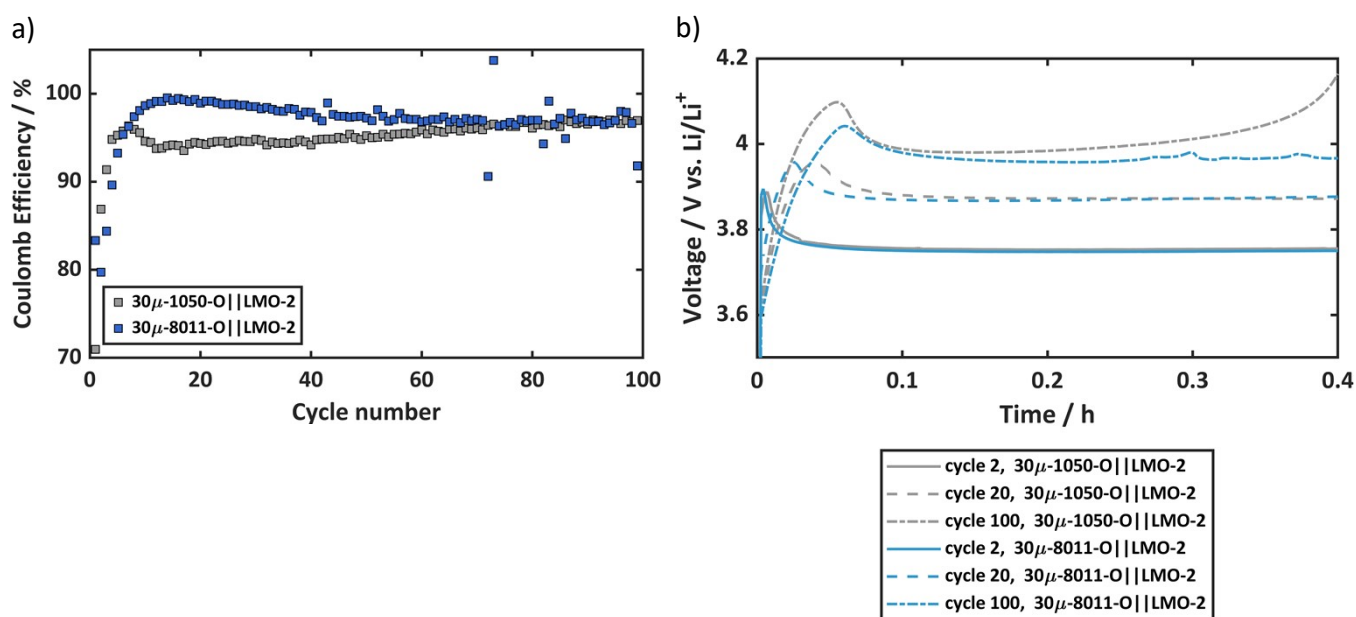


Figure S2: Relative discharge capacity over the number of cycles using the two different Al foil compositions high-purity Al 1050 and Fe and Si containing 8011 Al alloy in the same temper condition O and thickness in the full-cell set up $30\mu\text{-1050-O}||\text{LMO-2}$ vs. $30\mu\text{-8011-O}||\text{LMO-2}$. a) Coulomb efficiency over the number of cycles of the full-cells $30\mu\text{-1050-O}||\text{LMO-2}$ vs. $30\mu\text{-8011-O}||\text{LMO-2}$. b) Voltage profiles at the onset of the charging phase of cycle 2, cycle 20 and cycle 100 over time of the full-cells $30\mu\text{-1050-O}||\text{LMO-2}$ vs. $30\mu\text{-8011-O}||\text{LMO-2}$.

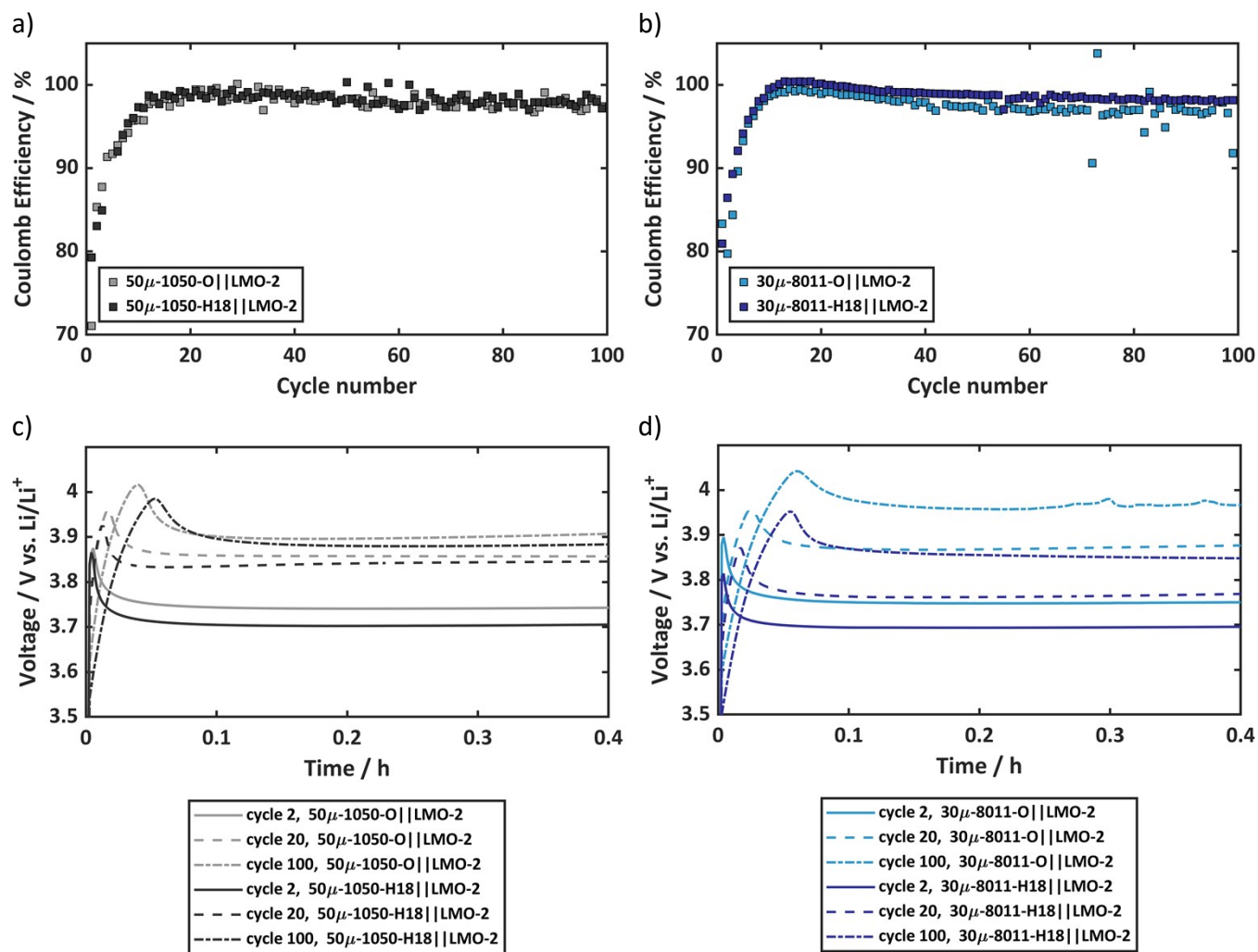


Figure S3: Graphs for the comparison between two different hardness levels represented by the tempers annealed O and strain-hardened H18 used on high-purity Al 1050 and Al alloy 8011. a) Coulomb efficiency over the number of cycles of the full cells 50μ-1050-O||LMO-2 and 50μ-1050-H18||LMO-2. b) Coulomb efficiency over the number of cycles of the full-cells 30μ-8011-O||LMO-2 and 30μ-8011-H18||LMO-2. c) Voltage profiles at the onset of the charging phase of cycle 2, cycle 20 and cycle 100 over time of the full-cells 50μ-1050-O||LMO-2 and 50μ-1050-H18||LMO-2. d) Voltage profiles at the onset of the charging phase of cycle 2, cycle 20 and cycle 100 over time of the full-cells 30μ-8011-O||LMO-2 and 30μ-8011-H18||LMO-2.

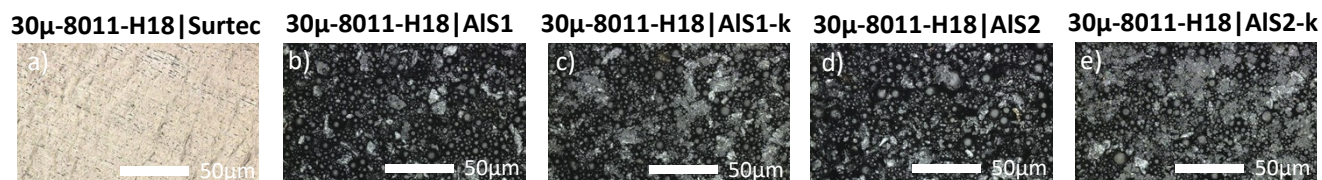


Figure S4: LSM images of the surface of the coated Al foils. a) 30μ-8011-H18|Surtec. b) 30μ-8011-H18|AIS1. c) 30μ-8011-H18|AIS1-k. d) 30μ-8011-H18|AIS2. e) 30μ-8011-H18|AIS2-k.

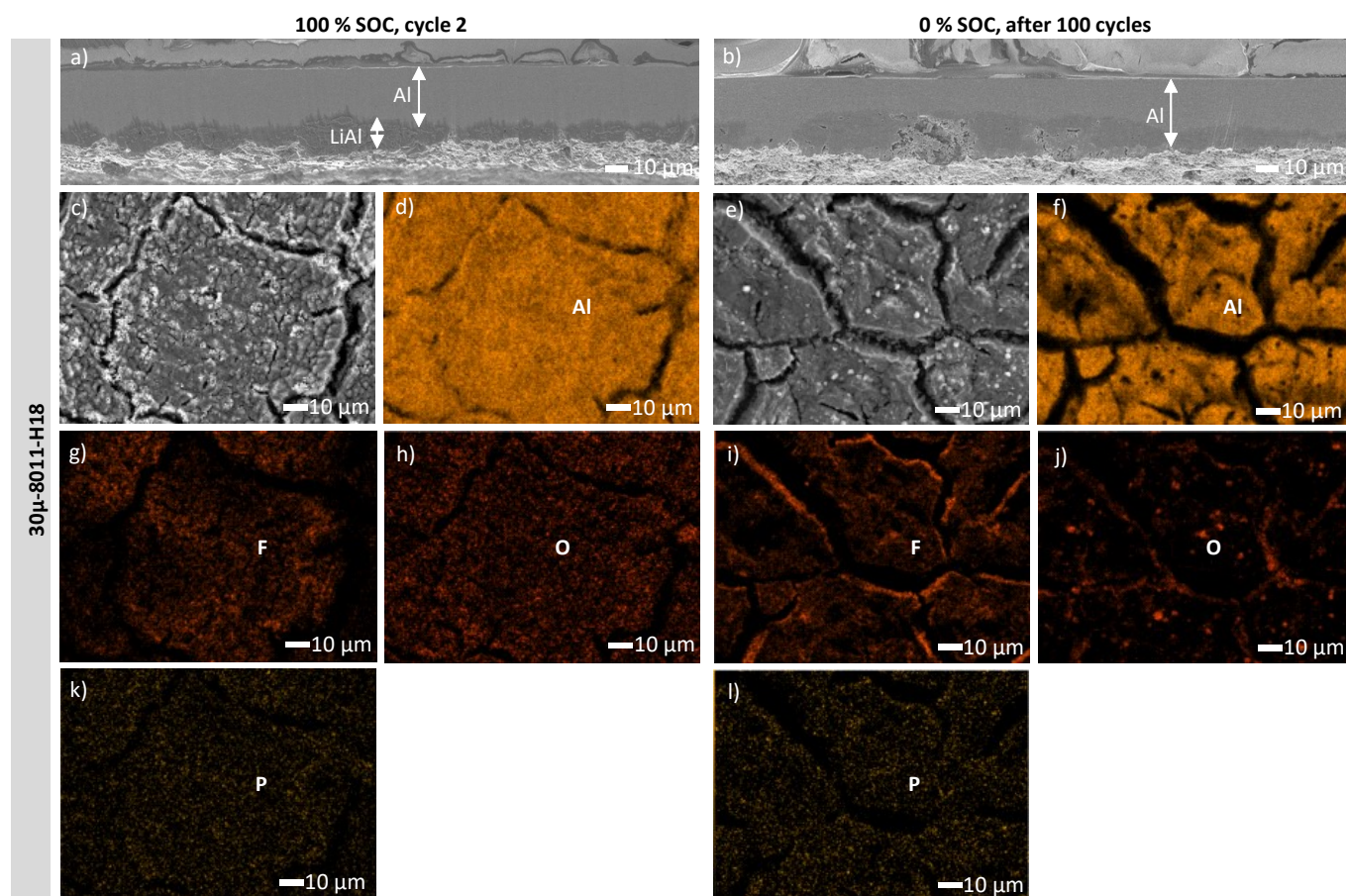


Figure S5: SEM image and EDX mapping of uncoated 30μ-8011-H18 used as anode in a full cell set up with LMO-2 cathode in the cycle condition 100 % SOC in cycle 2 and 0 % SOC after 100 cycles. a)/b) SEM image of the cross-section at 100 % SOC in cycle 2 and at 0 % SOC after 100 cycles. The lithiated side of the Al foil is at the lower edge of the foil. c)-l) EDX mapping of the surface top view at 100 % SOC in cycle 2 and at 0 % SOC after 100 cycles.

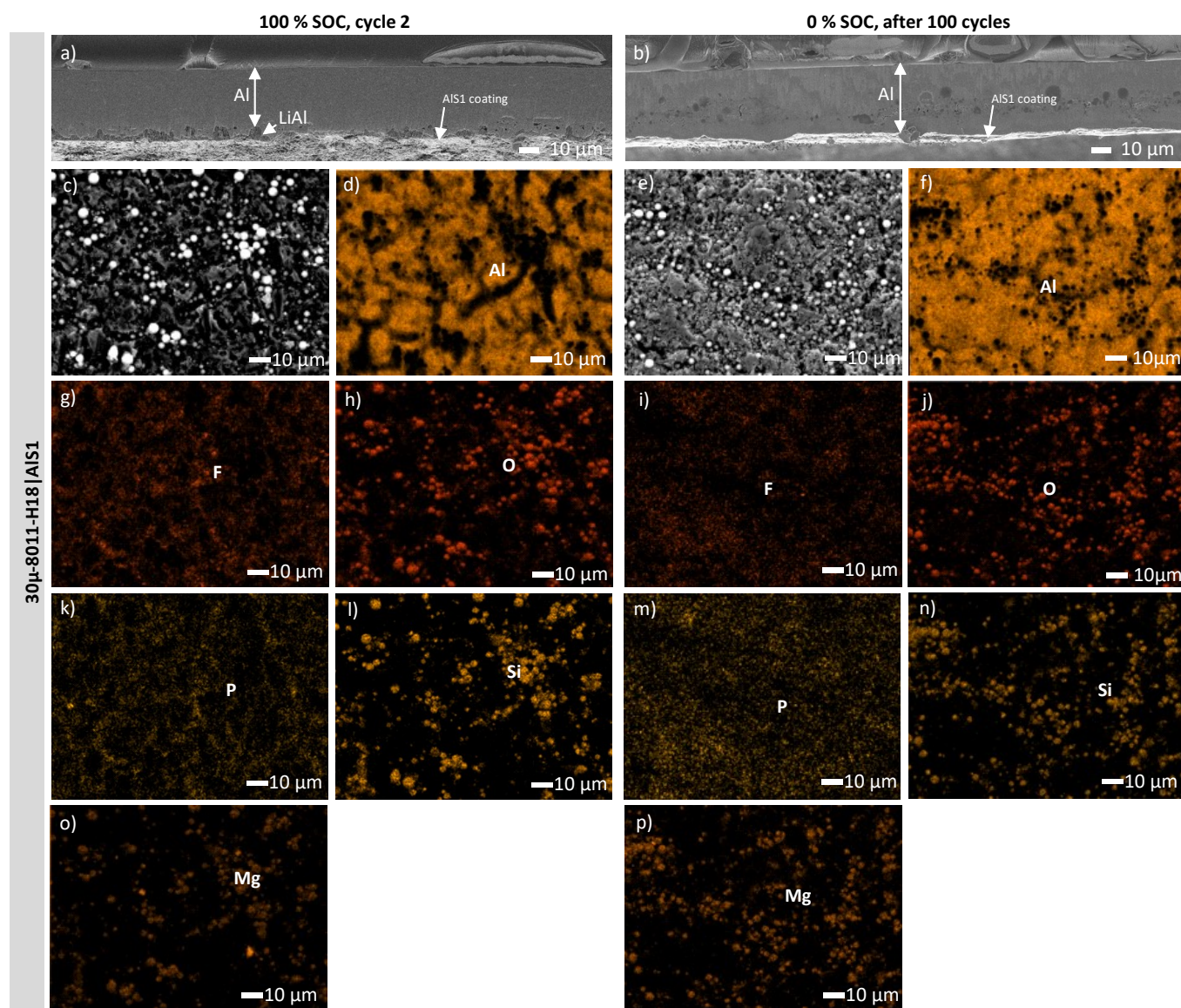


Figure S7: SEM image and EDX mapping of 30μ-8011-H18|AlS1 used as anode in a full cell set up with LMO-2 cathode in the cycle condition 100 % SOC in cycle 2 and 0 % SOC after 100 cycles. a)/b) SEM image of the cross-section at 100 % SOC in cycle 2 and at 0 % SOC after 100 cycles. The lithiated side of the Al foil is at the lower edge of the foil. c)-l) EDX mapping of the surface top view at 100 % SOC in cycle 2 and at 0 % SOC after 100 cycles.

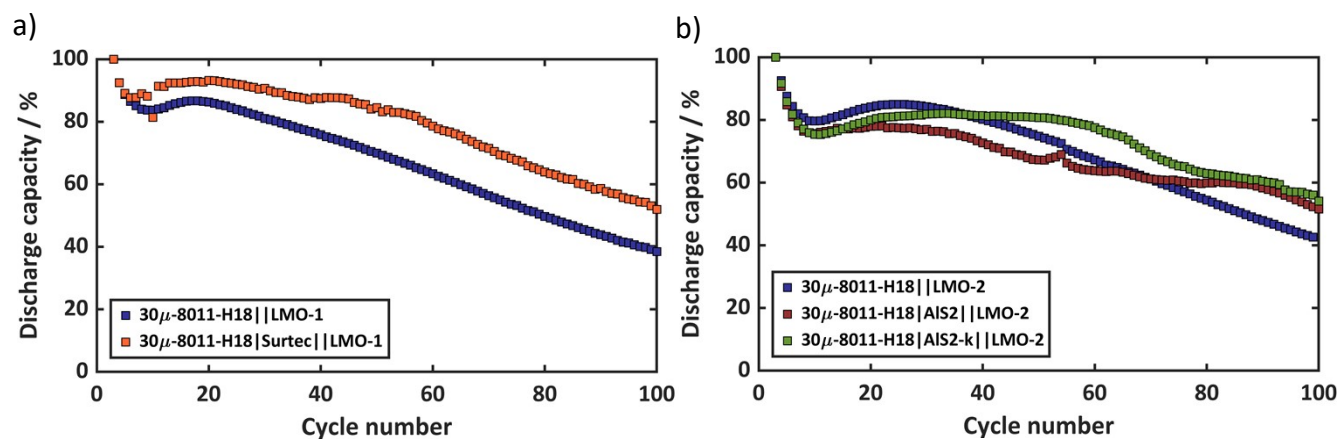


Figure S8: Graphs for the analysis of the influence of using an inert, ion conducting passivation layer coated on the Al foil. The full-cell set ups $30\mu\text{-8011-H18}||\text{LMO-1}$ and $30\mu\text{-8011-H18}||\text{LMO-2}$ are used as reference. a) Relative discharge capacity over the number of cycles of the full cell using a Cr(III) passivation layer (Surtec): $30\mu\text{-8011-H18}|\text{Surtec}||\text{LMO-1}$. b) Relative discharge capacity over the number of cycles of the full cells using an uncalendered Al silicate (AIS) and a calendered Al silicate (AIS-k) coating: $30\mu\text{-8011-H18}|\text{AIS2}||\text{LMO-2}$, $30\mu\text{-8011-H18}|\text{AIS2-k}||\text{LMO-2}$. Cycling data is presented as the mean value of two representative cells for each configuration.